Extended Data 1. Solution-state absorbance and photoluminescence spectra

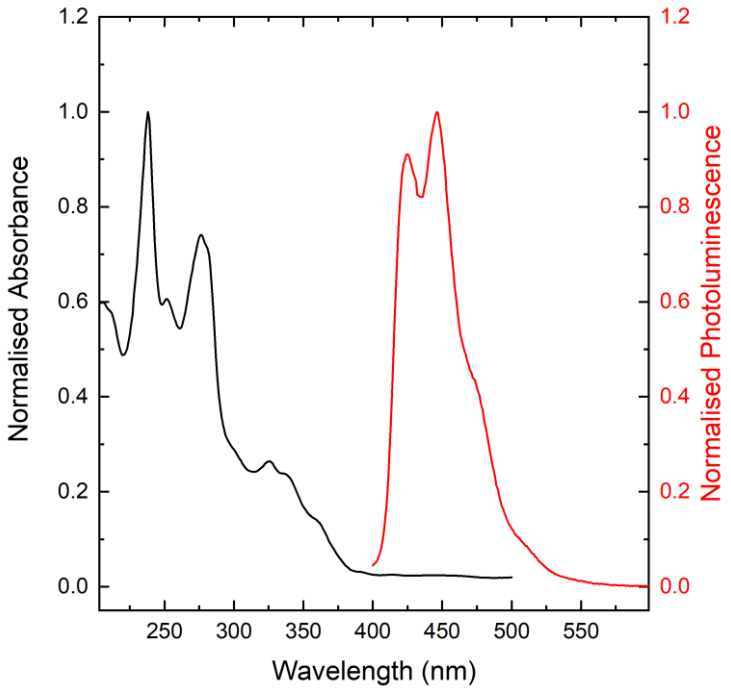

Absorption and photoluminescence spectra of CN6H in acetonitrile ($2 \cdot 10^{-5}$M). *The excitation wavelength was 325 nm.*

Extended Data 2. UV-Visible absorption and circular dichroism of neat templating layers

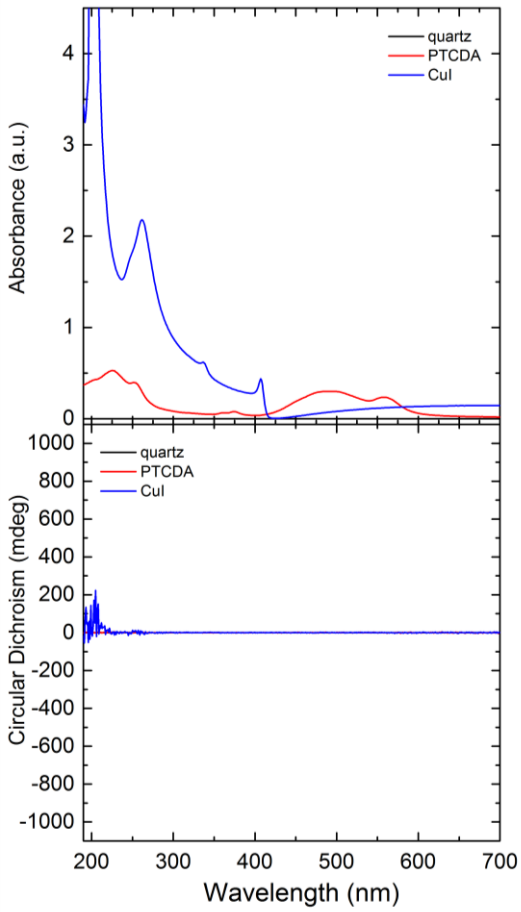

UV-Vis and Circular Dichroism of the templating layers (PTCDA: 20 nm, CuI: 100 nm).

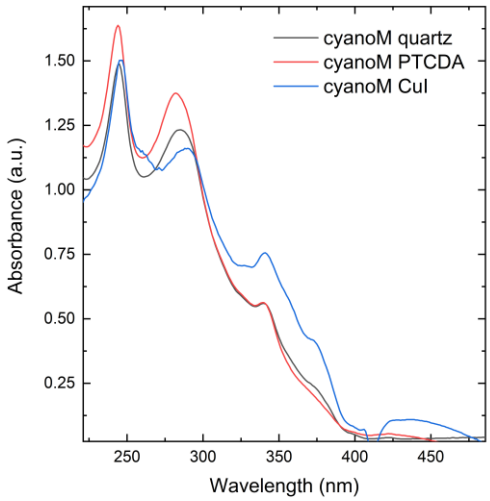

UV-Vis of CN6H [M] thin films subtracting the absorbance of the templating layers.

Extended Data 3. UV-Visible absorption and photoluminescence spectra of CN6H thin films

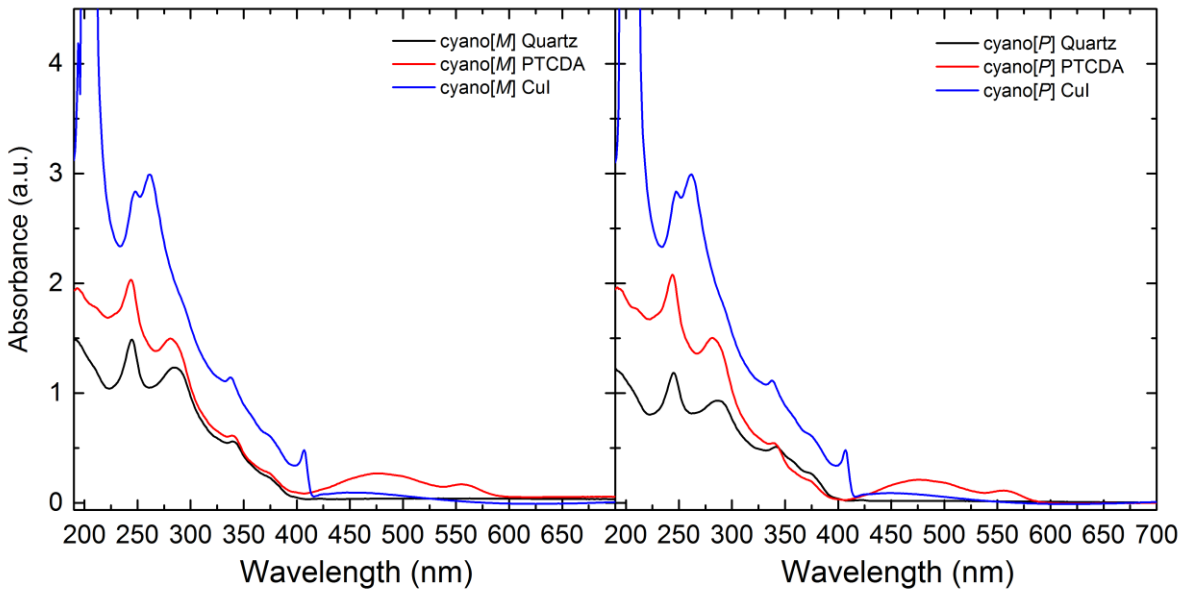

UV-visible absorption spectra of CN6H thin films (thickness: 78 nm) on a non-interacting substrate (quartz, black line), 20 nm PTCDA (red) and 100 nm CuI (111) (blue line).

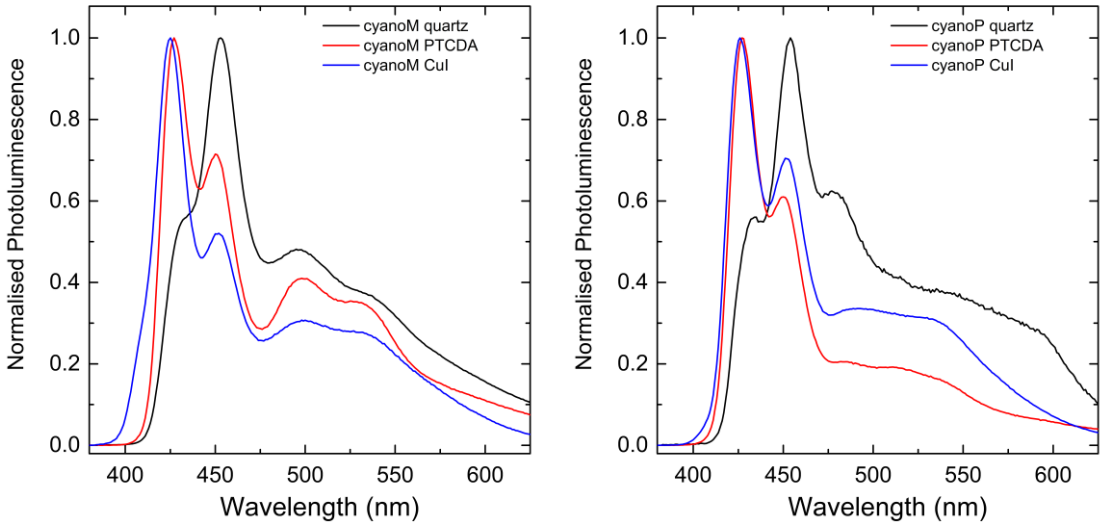

Photoluminescence spectra of CN6H thin films (thickness: 78 nm) on a non-interacting substrate (quartz, black line), 20 nm PTCDA (red) and 100 nm CuI (111) (blue line). The excitation wavelength was 325 nm.

Extended Data 4. XRD of CN6H [*P*] thin films

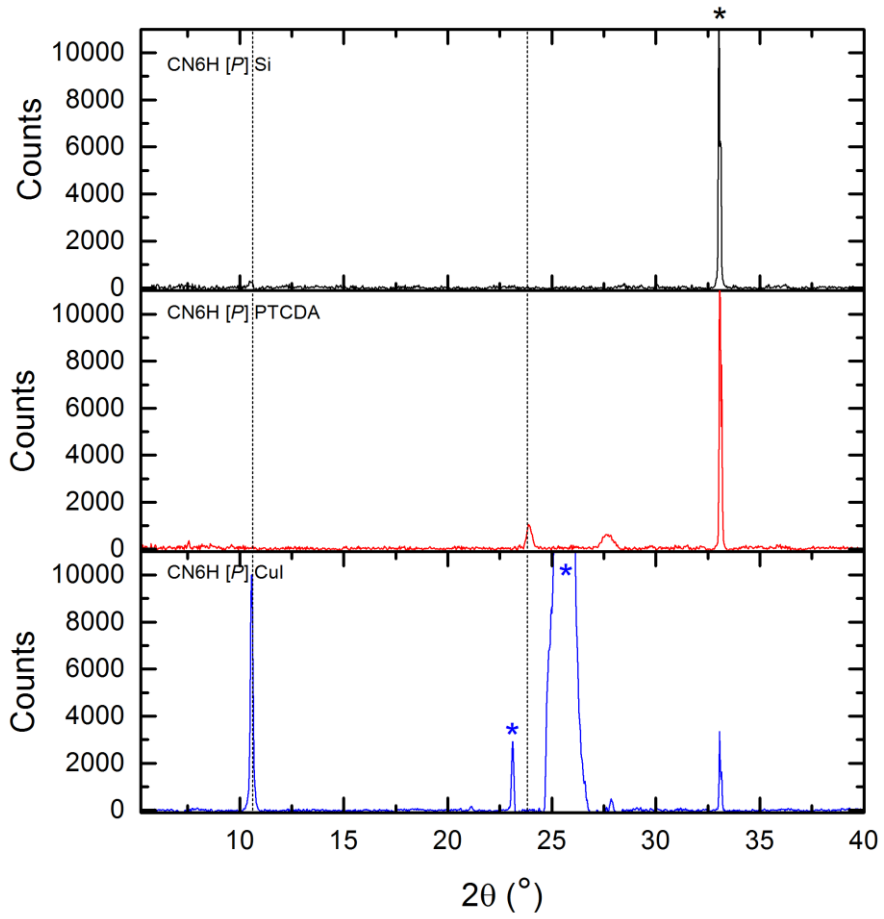

X-Ray diffraction of CN6H thin films (thickness: 78 nm) on a non-interacting substrate (quartz, black line), 20 nm PTCDA (red) and 100 nm CuI (111) (blue line).

Extended Data 5. Atomic force microscopy of CN6H thin films

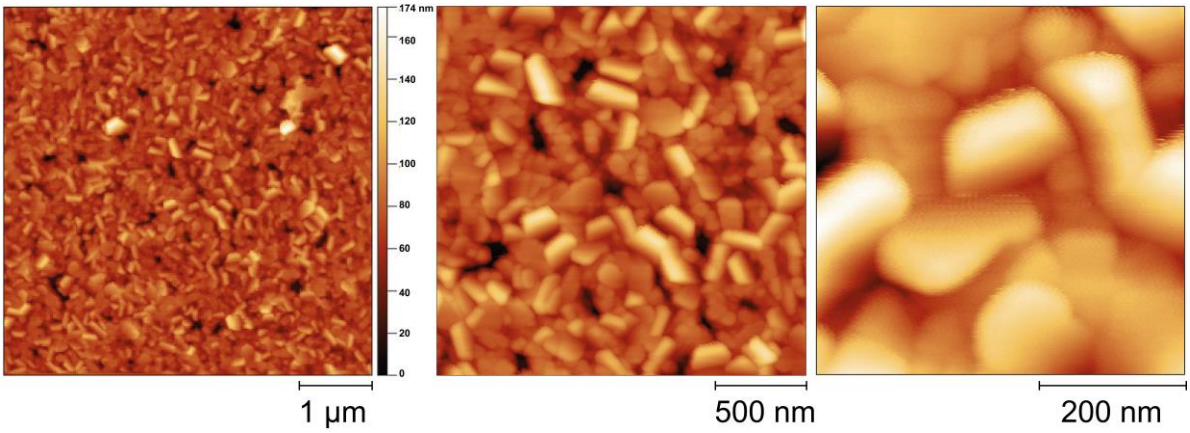

*Atomic force microscopy images of CuI-templated **CN6H** [M]. The scale bar is indicated.*

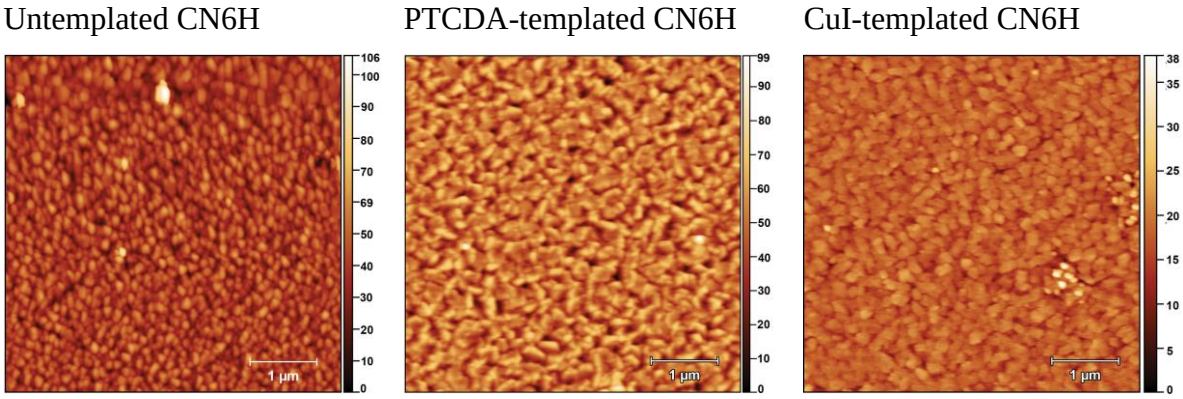

*Atomic force microscopy images of untemplated and templated **CN6H** [P]. The scale bar is 1 µm.*

We note that the topography of the neat templating layers has been reported elsewhere, with surfaces of the 100 nm CuI thin films featuring large, pinhole free smooth grains.[25] Unfortunately, the neat PTCDA layers are too sticky to successfully image. These types of strong interactions contribute to the broad distribution of supramolecular columns orientations illustrated in Figure 3.

Extended Data 6. Planar and cross-sectional view scanning electron microscopy

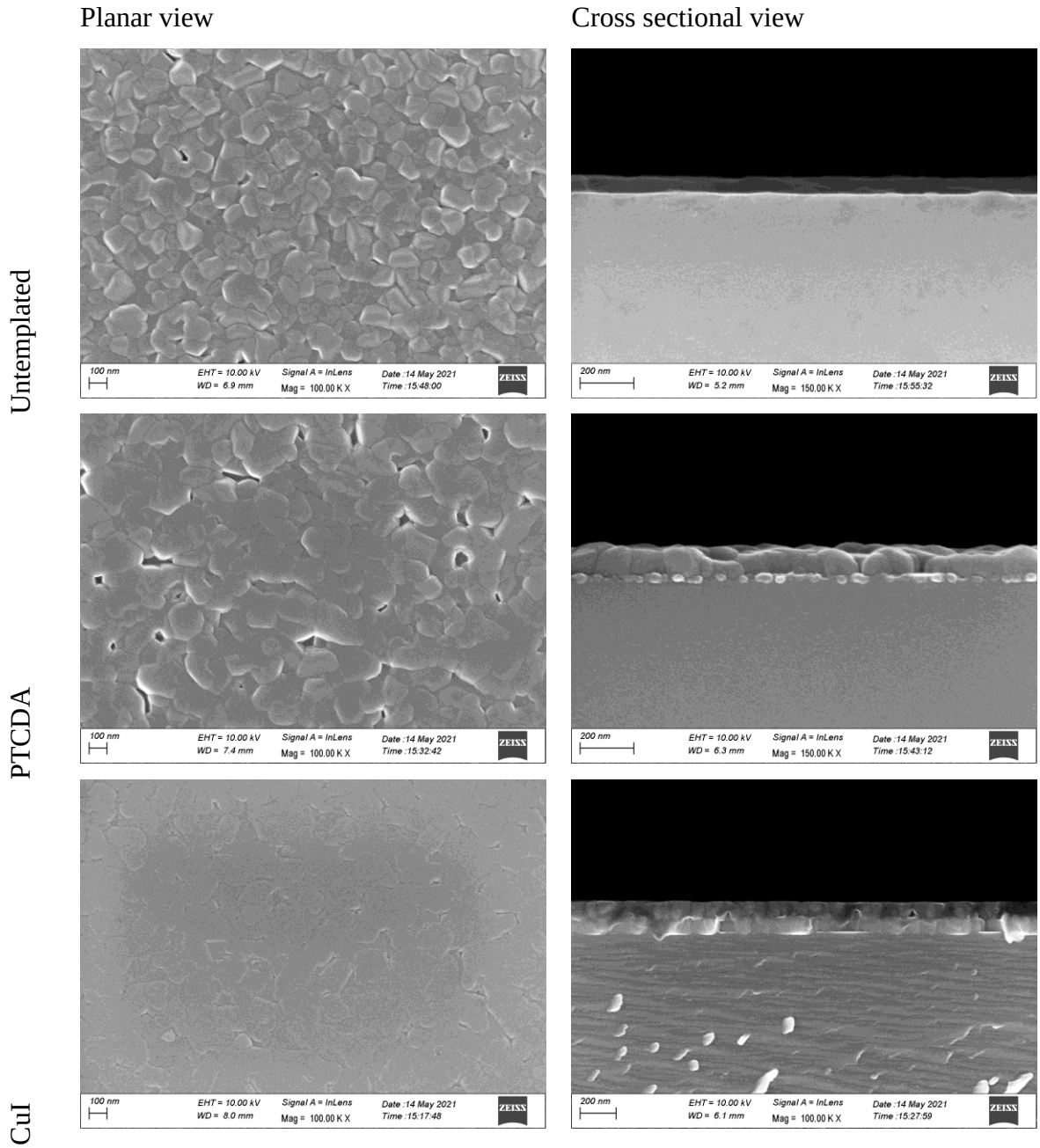

The dramatically different morphologies are also apparent in cross-sectional view SEM: in particular, the smooth surface of the flat-lying supramolecular columns of CuI-templated **CN6H** and uneven, rough surfaces of PTCDA-templated **CN6H**. Remarkably, PTCDA-templated **CN6H** appears to form molecular clusters in domains that extend throughout the entire film thickness, whilst there is some evidence of a layering in the platelet-packing on CuI. The ultra-smooth films of CuI-templated **CN6H** is responsible for the poor contrast in the planar view SEM.

Extended Data 7. CN6H [*P*] 2D GIWAXS patterns and simulations

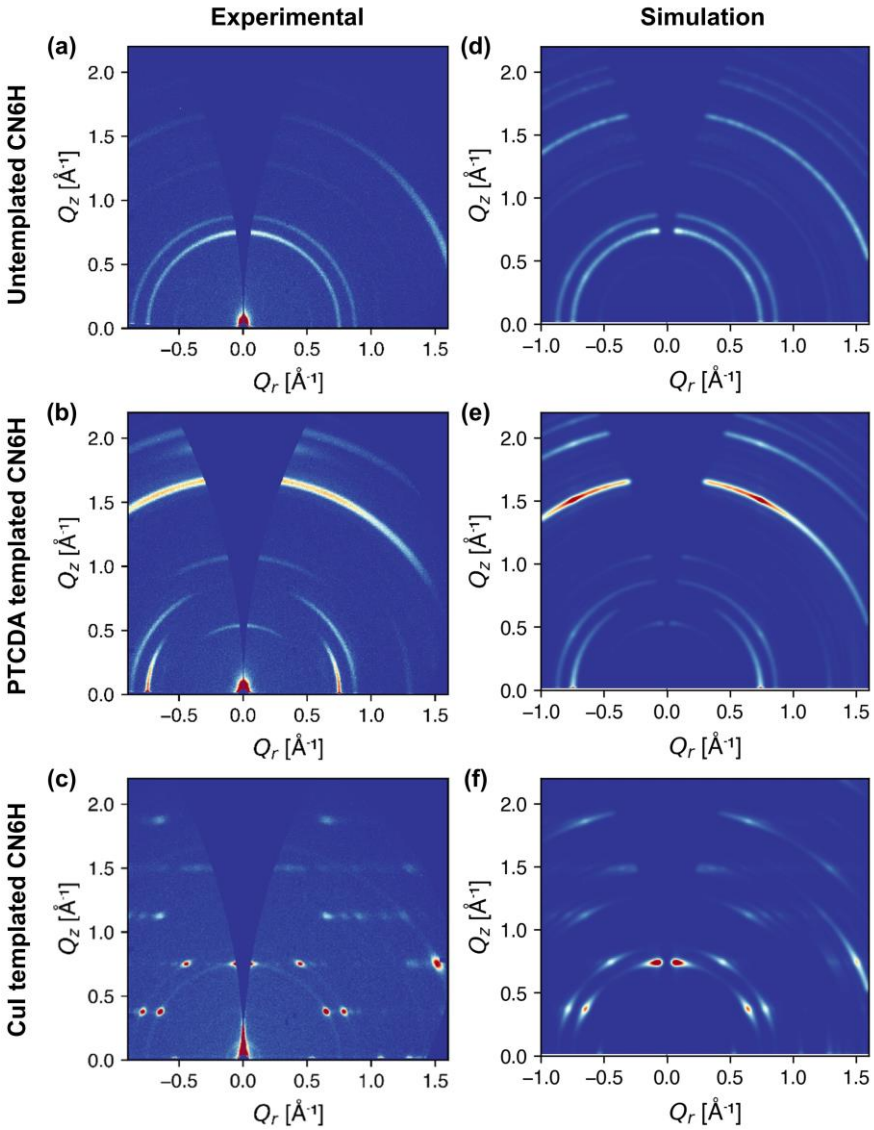

*Experimental and simulated two-dimensional (2D) GIWAXS diffraction patterns of untemplated and templated **CN6H** [P].*

In contrast to **CN6H** [M], the 1 0 0 reflection of untemplated **CH6H** [P], has a stronger out-of-plane intensity and the experimentally observed 2D GIWAXS pattern can be replicated by simulating a broad distribution with (1 0 0) planes parallel to the substrate. For PTCDA-templated **CH6H** [P], the scattering intensity is stronger compared to **CN6H** [M] but the 2D GIWAXS patterns of both enantiomers can be replicated by simulating a face-on arrangement of supramolecular columns with a reasonably broad distribution of crystallite orientations. CuI-templated **CN6H** [P] exhibits smaller Bragg spots compared to **CN6H** [M] but both enantiomers exhibit edge-on orientation and are simulated using the same uniaxial model. We attributed the small differences between **CN6H** [P] and [M] to experimental variations. Part (f) is repeated from Figure 3f.

Extended Data 8. Azimuthally integrated Q-dependent 1D intensity profiles

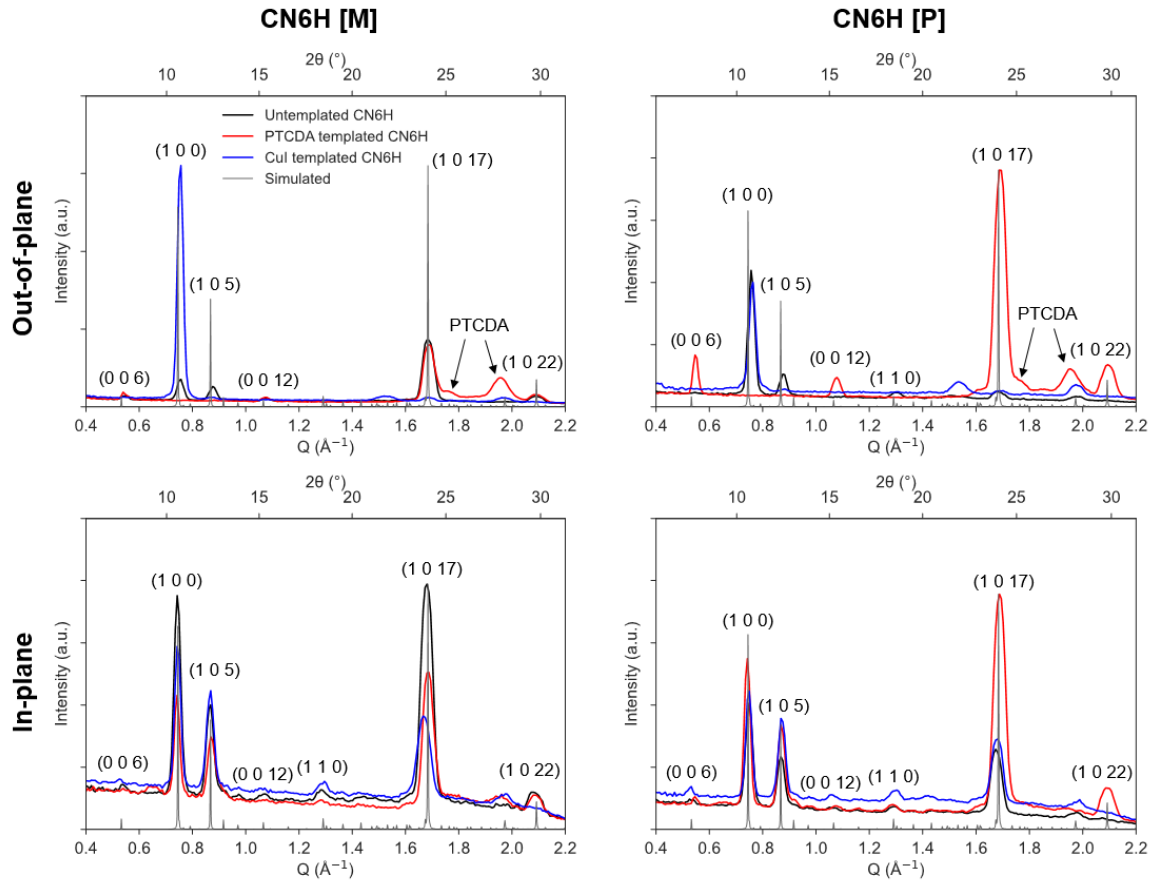

*Azimuthally integrated Q-dependent 1D intensity profiles of untemplated and templated **CN6H** [M] and **CN6H** [P], integrated in the range 0.2 Å^{-1} ≤ Q ≤ 2.2 Å^{-1} through various χ angles; out-of-plane (in the Qz direction, χ= 0°±20°) and in-plane (which includes all other angles 20° ≤ χ ≤ 90°). The simulated powder XRD from Supplementary Figure 2 is overlayed and the highest intensity reflections are labelled with the correpsonding Miller indices. We attribute the small differences between **CN6H** [M] and **CN6H** [P] to experimental variations.*

Extended Data 9. Proposed mechanism for PTCDA templating

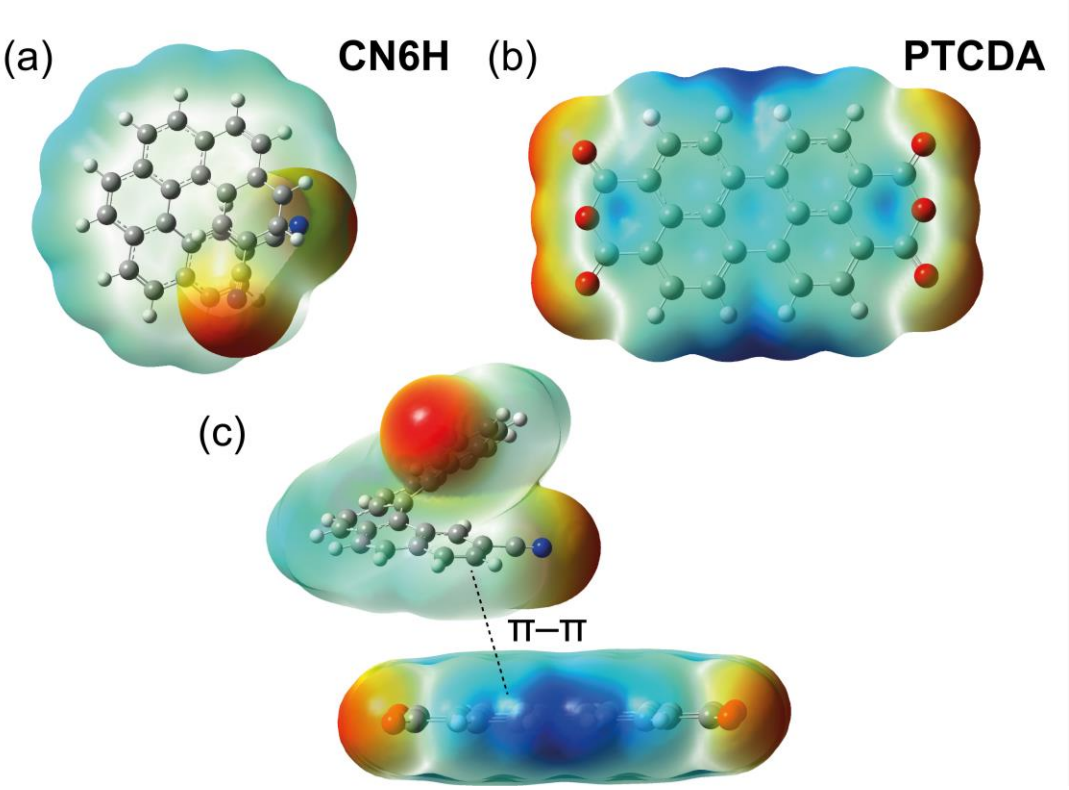

Theoretical molecular electrostatic potential surfaces (a) ***CN6H*** *and (b) PTCDA calculated using DFT using the B3LYP hybrid functional at the 6-311G(d,p) level of theory. The red areas represent electron rich regions of the molecule, whilst the blue areas represent electron poor regions. (c) a cartoon depicting the* $\pi - \pi$ *interactions of flat-lying PTCDA and* ***CN6H****.*

Extended Data 10. Proposed mechanism for CuI templating

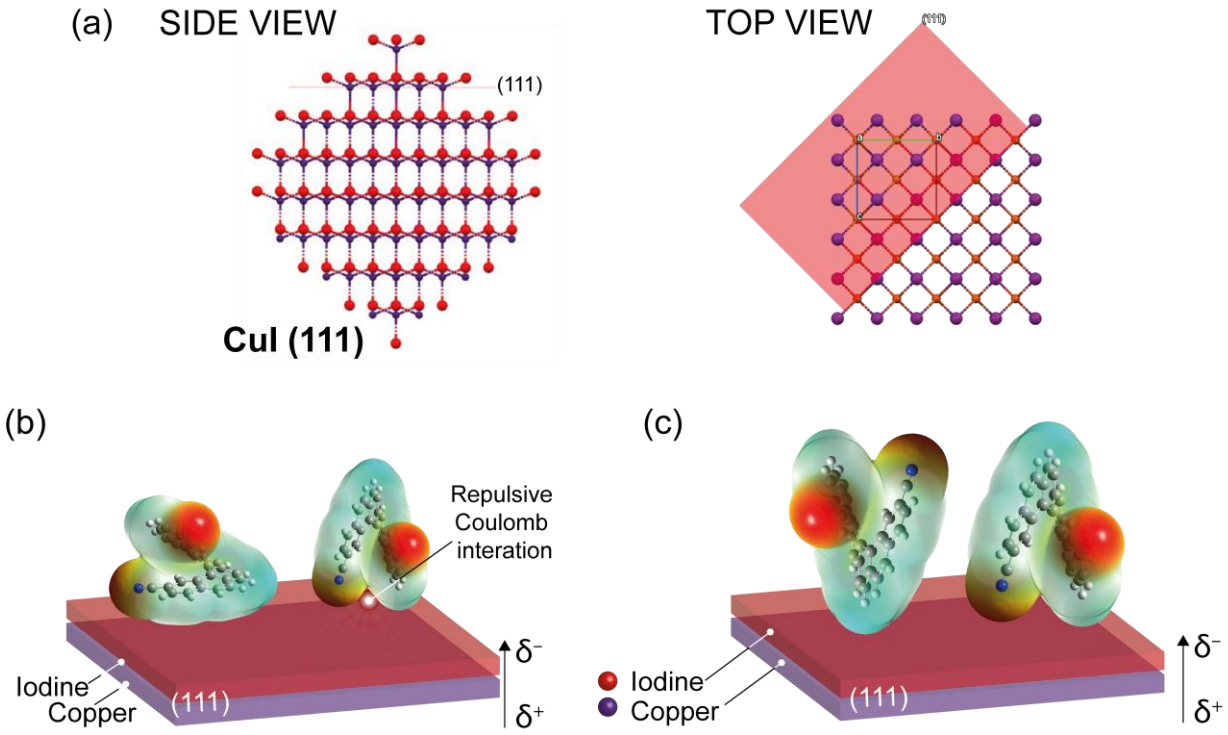

(a) Side and top-view of the crystal packing of CuI along the (111) plane, showing the relative positions of the iodine and copper atoms. The surface primarily consists of iodine atoms. (b) and (c) Theoretical molecular electrostatic potential surfaces of ***CN6H*** *and a cartoon of the electrostatic interactions that force the edge-on configuration of* ***CN6H*** *on CuI.*